ELSEVIER

Chemical Engineering Journal 137 (2008) 38–44

Chemical Engineering Journal

www.elsevier.com/locate/cej

Comparative study of solid silica nanoparticles and hollow silica nanoparticles for the immobilization of lysozyme

Qing-Gui Xiao [b], Xia Tao [a], Hai-Kui Zou [b], Jian-Feng Chen [a,b,*]

[a] *Key Lab for Nanomaterials of the Ministry of Education, Beijing University of Chemical Technology, Beijing 100029, China*
[b] *Research Center of the Ministry of Education for High Gravity Engineering & Technology, Beijing University of Chemical Technology, Bei San Huang Dong Road 15, Beijing 100029, China*

Received 30 May 2007; received in revised form 7 August 2007; accepted 3 September 2007

Abstract

In this study, three different morphology silica materials, i.e. hollow silica nanotubes, hollow silica nanospheres and solid silica nanoparticles were prepared and then employed as supports for immobilization of lysozyme. The produced silica materials were characterized by transmission electron microscopy (TEM), FTIR and BET. The comparative study of three silica materials for the immobilization of lysozyme indicated that the amount of immobilized lysozyme on solid silica nanoparticles was 186 mg/g silica, and while that of immobilized lysozyme within hollow silica nanotubes and hollow silica nanospheres could, respectively, reach up to 351 mg/g silica and 385 mg/g silica. Among the three types of silica supports, it was obvious that the hollow silica nanospheres represented the highest immobilization ability, whereas the specific activity of immobilized lysozyme on silica nanospheres (1.38×10^6 unit/g) was slightly lower than that of immobilized lysozyme on silica nanotubes (1.46×10^6 unit/g). This unexpected phenomenon is more likely to be due to the relatively airtight structure of hollow silica nanospheres. Compared to solid silica nanoparticles, silica materials with hollow structure and large pore size would facilitate the enzymatic immobilization.

Keywords: Lysozyme immobilization; Silica nanospheres; Silica nanotubes; Enzymatic activities

1. Introduction

The immobilization of enzymes on solid supports is an area of intense research due to the widespread application of immobilized enzymes in synthetic chemistry and industry [1–3]. In this field, a central requirement for consolidating biocatalysis is the development of supports and immobilization methods capable of providing cheap, stable, efficient heterogeneous biocatalysts [4]. As conventional supports for the immobilization of enzymes, polymeric organic materials have a low reusability. In recent years, inorganic materials with large specific surface area and unique structure have drawn growing interest of researchers [5,6]. Among inorganic materials, silica materials for the immobilization of enzymes have been explored extensively because they are environmentally more acceptable, structurally more stable and chemically more resistant to organic solvents and microbial attacks [4,7–9]. Silica materials with different morphologies such as monoliths, films, rod-like particles, fibers, hollow nano/microspheres and hollow nanotubes also have been fabricated [10–13]. Takahashi et al. [14,15] have reported the ordered mesoporous silica (MCM-41, FSM-16 and SBA-15) for the immobilization of horseradish peroxide. Mann and co-workers [16] have synthesized silica fibers with triangular or rectangular-shaped channels by coupling TEOS hydrolysis/condensation reactions in situ crystallization of ammonium oxalate.

Since the pioneering works on the fabrication of hollow spheres were performed by Kowalski et al. [17], hollow spheres and tubes with well-defined structures have been attracting interest in the area of materials research. Recently, a variety of chemical and physicochemical methods have been investigated, including emulsion/interfacial polymerization strategies [18,19], heterophase polymerization combined with a sol–gel process [20,21], self-assembly techniques [22,23] and surface living polymerization processes [24,25]. Lin and co-workers [26] have reported that hollow silica spheres with

* Corresponding author at: Key Lab for Nanomaterials of the Ministry of Education, & Research Center of the Ministry of Education for High Gravity Engineering & Technology, BUCT, Beijing 100029, China.
Fax: +86 10 64434784.
E-mail address: chenjf@mail.buct.edu.cn (J.-F. Chen).

1385-8947/$ – see front matter © 2007 Published by Elsevier B.V.
doi:10.1016/j.cej.2007.09.012

mesostructured shell were prepared with a vesicle template of cetyltrimethylammonium bromide-sodium dodecyl sulfate-pluronic following a fast silicification in dilute silicate solution and found that the mesostructure of the shell is disordered and the mesopore size is about 5.5–7.5 nm. Wu and co-workers [27] have performed a novel method for the fabrication of small monodisperse hollow silica spheres, and in this approach, when silica shells were coated on polystyrene particles by the sol–gel method, the polystyrene cores were dissolved subsequently, even synchronously, in the same medium to form monodisperse hollow spheres. Furthermore, the formation of hollow silica nanotubes has been reported by many researchers. Murphy and co-workers [28] have synthesized the hollow silica nanotubes through dissolution of the Au core from the silica-coated Au nanorods. Martin and co-workers [29] have also synthesized the hollow silica nanotubes within the pores of nanopore alumina template membranes using a sol–gel method. These hollow nanoparticles have a number of excellent properties that make them potential candidates for enzyme immobilization. First, they have inner voids that can be filled with species ranging in size from large proteins to small molecules. In addition, they have distinct inner and outer surfaces that can be differentially functionalized. Finally, the mesostructure of the shells with the tunable pore size and pore distribution allows small molecules and ions to diffuse into or out off the hollow nanoparticles, producing shorter diffusion path lengths.

In this paper, solid silica nanoparticles, hollow silica nanospheres and hollow silica nanotubes were synthesized for enzyme immobilization. Three silica nanoparticles with different morphologies possess the same surface groups, i.e. Si–OH groups, as evidenced by FTIR. Lysozyme was employed as a representative enzyme to investigate its adsorption behavior on three types of silica materials at neutral pH. We found that the adsorption process of lysozyme onto hollow silica materials could be divided into two stages. In addition, effects of support morphology on the loading of lysozyme and on the catalytic activity of the immobilized enzymes will be also discussed in this work.

2. Experimental

2.1. Chemicals

Solid silica nanoparticles, hollow silica nanospheres and hollow silica nanotubes were synthesized by our group [20,30]. Lysozyme, a small globular protein with an approximate diameter of 3 nm and isoelectric point without specific ionic adsorption at 11.4 [31], was obtained from a commercial source (Fluka Co.). All chemicals were reagent grade and used without further purification. Deionized water was prepared with an ion exchange system.

2.2. Fabrication of silica nanoparticles

Solid silica nanoparticles were obtained in high-gravity environment generated by rotating packed bed reactor. Hollow silica nanospheres with a porous shell structure were fabricated via the sol–gel method and using cuboidal $CaCO_3$ nanoparticles as inorganic templates [20,32]. Hollow silica nanotubes with a porous shell structure were also synthesized via a similar method using needle-like $CaCO_3$ nanoparticles as inorganic templates [33].

2.3. Immobilization of lysozyme on silica nanoparticles

The immobilization process of lysozyme onto silica nanoparticles was illustrated in Fig. 1. The as-prepared solid silica nanoparticles, hollow silica nanospheres and hollow silica nanotubes, under constant stir, were added into lysozyme solution (1 mg/mL), respectively. At different time intervals 5 mL of the suspensions were withdrawn and immediately centrifuged to obtain clear supernatant, which was used to determine the residual lysozyme concentration by a UV spectrometer at a wavelength of 280 nm. The amount of lysozyme immobilized onto silica nanoparticles was calculated from the original lysozyme concentration and the amount of lysozyme in the supernatant after adsorption. After the adsorption had reached the equilibrium, the suspension was filtered and rinsed with deionized water to remove untrapped lysozyme molecules. Samples of lysozyme immobilized onto silica nanoparticles were dried and kept in stock for subsequent enzyme activity assay.

2.4. Measurement of the enzyme activity

The activity of lysozyme immobilized in silica nanoparticles was measured by a standard assay procedure. Micrococcus was selected as the substrate to examine the catalytic capability of lysozyme, which was correlated to the degradation rate of micrococcus in the presence of lysozyme. The substrate was dispersed in a phosphate solution of pH 6.5 in a cuvette and the as-prepared suspension was monitored by a UV spectrometer to determine the degradation rate of micrococcus via the variation of UV absorbance. The suspension was in stock for enzymatic activity examination while the UV absorbance at 450 nm reached approximately 1.3. Then either free lysozyme or lysozyme-immobilized silica nanotubes, dissolved or dispersed, respectively in phosphate buffers, were added into micrococcus suspension and the decrease of the UV absorbance at 450 nm was recorded for the initial 5 min. The plot of enzymatic activities versus different loading amount of lysozyme was thus established, and each run of activity measurements was carried out four times and the average value was adopted in this experiments.

2.5. Apparatus

TEM (HITACHI, H-800) was used to study the morphology and structures of the silica samples. The concentration of lysozyme solution was determined by a Shimadzu UV 2501 spectrometer at an absorption wavelength of 280 nm. Zeta potentials of solid and hollow silica materials were measured by a MALVEN ZETASIZER-3000HS. BET surface area, pore volume and pore size of the samples was determined from N_2 adsorption–desorption isotherms obtained at 77 K using an ASAP 2010 Surface Area Analyzer. Prior to measurement, all samples were outgassed at 473 K and 0.1 Pa for 2 h.

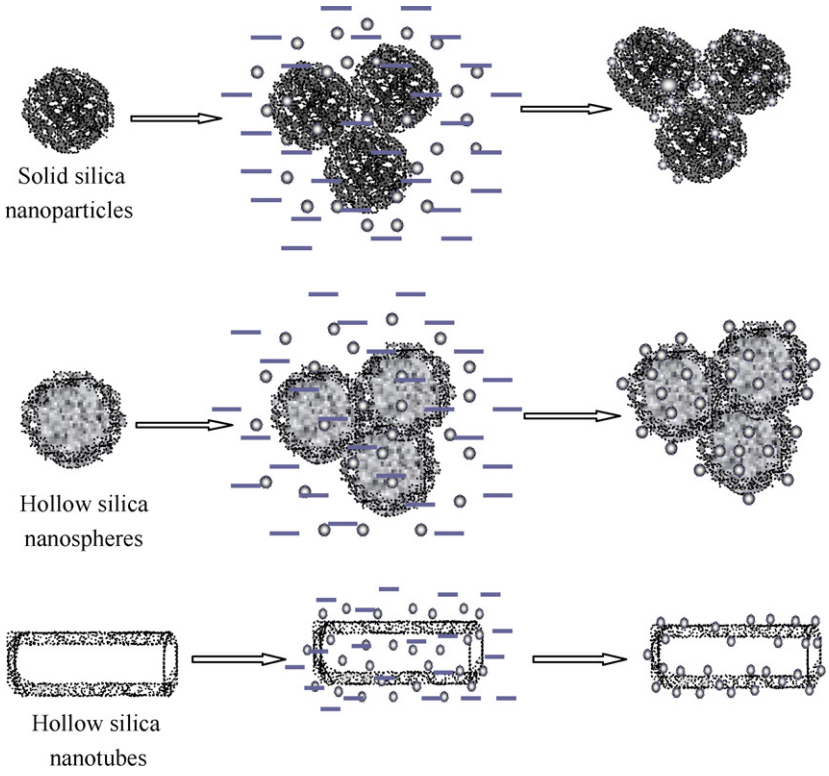

Fig. 1. Schematic illustration of immobilization of lysozyme from aqueous solution onto solid silica nanoparticles and hollow silica nanoparticles.

3. Results and discussion

3.1. Analyses of morphology and size of silica materials

Fig. 2 shows the morphology and size of as-prepared $CaCO_3$ templates and silica nanoparticles. Fig. 2a indicated solid silica nanoparticles with the size of ca. 20–30 nm. The shape and size of the inner space of hollow silica nanotubes can be determined directly by the shape and size of needle-like $CaCO_3$ templates (Fig. 2b). The average inner diameter of silica nanotubes (SNT) in the middle and at the closed ends (Fig. 2c) was 200–250 and 50–60 nm, respectively. It was worth noting that most of the as-prepared hollow silica nanotubes are open at one or two ends, and thus provide more entrance for immobilization of enzyme. Also, the walls of the nanotubes were uniform and smooth, and had a thickness of about 30–40 nm, which could be controlled by the $SiO_2/CaCO_3$ ratio during the preparation. In fact, the existence of big openings at the nanotubes ends would allow the large internal void space to trap macromolecules or larger entities, which will be practically applicable in many applications such as bio-immobilization and functional materials. The silica nanospheres (Fig. 2e and f) were synthesized through using cuboidal $CaCO_3$ nanoparticles (Fig. 2d) as inorganic templates, and the size of hollow silica nanospheres was 80–150 nm.

The typical nitrogen adsorption isotherm at 77 K for the silica materials and their pore size distribution determined by a Micromeritics ASAP2010 Analyzer are shown in Fig. 3 (for solid silica nanoparticles), in Fig. 4 (for hollow silica nanotubes) and in Fig. 5 (for hollow silica nanospheres), respectively. Fig. 6 shows the variation of zeta potential for the silica materials with the pH value is similar. The physical properties of various silica materials are compiled in Table 1. According to the data in Table 1, three different morphology silica materials have a resemble zeta potential, slightly different pore volume (V_{pore}) and surface area (S_{BET}), while obviously different pore diameter (D_{pore}), which is convenient for us to investigate the effect on enzyme loading process from support structures.

3.2. FTIR analysis

Fig. 7 shows the FTIR analysis of the surface groups of the silica materials. 3430 cm^{-1} is the non-symmetric stretch-

Table 1
Physical properties of silica materials[a]

Sample	V_{pore} (cm^3/g)	D_{pore} (Å)	Zeta potential (mV)	S_{BET} (m^2/g)
Solid silica nanoparticles	1.08	12.6	−30.8	403.8
Hollow silica nanotubes	0.78	66.9	−31.9	458.5
Hollow silica nanospheres	0.93	55.8	−31.5	474.2

[a] Zeta potential values given here at pH 7 and the room temperature.

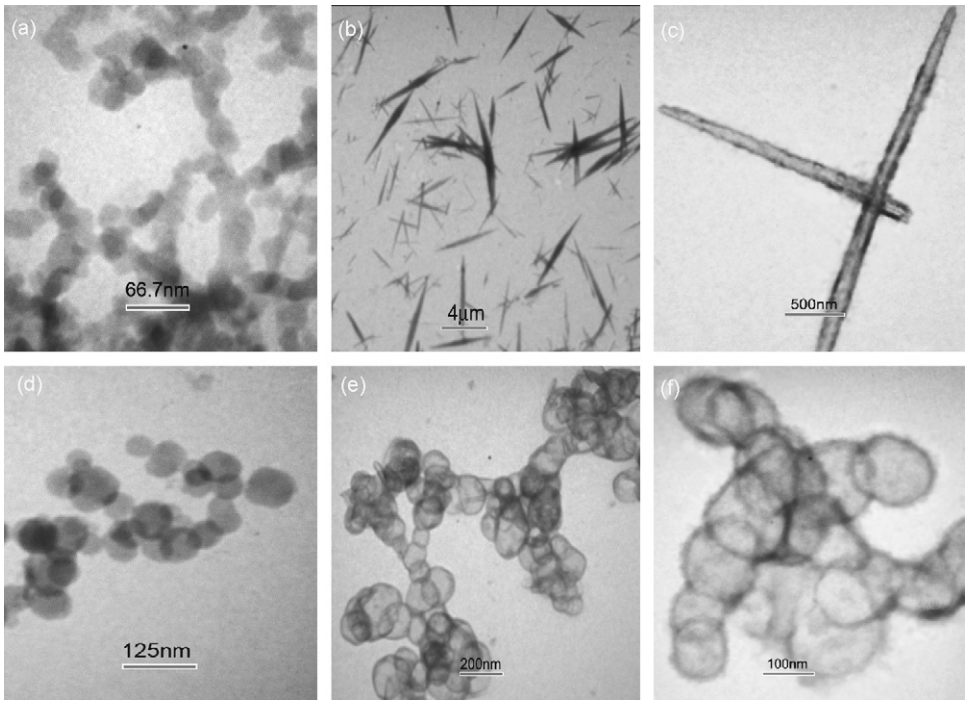

Fig. 2. TEM images of different nanoparticles: (a) solid silica nanoparticles; (b) needle-like $CaCO_3$ nanoparticles; (c) hollow silica nanotubes; (d) cuboidal $CaCO_3$ nanoparticles; (e) hollow silica nanospheres. A magnified TEM image of hollow silica nanospheres (f).

ing vibration of O–H groups bound with the surface of silica materials. 1630 cm^{-1} is the flexural vibration of H–O–H groups adsorbed onto the surface and channel of silica materials. 1100 and 800 cm^{-1} are the non-symmetric and symmetric stretching vibration of Si–O–Si groups, respectively. 957 cm^{-1} is the stretching vibration of Si–OH groups. It can be seen that the surface groups of the three samples are similar and mainly composed of Si–OH groups, which facilitates the interaction between the amino and/or carboxylic groups on the enzyme surface and the Si–OH groups on the silica materials surface via hydrogen-bonding [34].

In addition, Fig. 7 shows the FTIR spectra recorded from pure lysozyme (curve 4), lysozyme-immobilized solid silica nanoparticles (curve 5), lysozyme-immobilized hollow silica nanotubes (curve 6) and lysozyme-immobilized hollow silica nanospheres (curve 7). As it is well known, the amide linkages between amino acid residues in polypeptides and protein give the well-known fingerprints from the IR spectrum [35]. The position of the amide I and II bands in the FTIR spectra of proteins is a sensitive indicator of conformational changes in the protein secondary structure [36] and have been used in the study to investigate the immobilized enzymes molecules. The amide I peak at about 1650 cm^{-1} can be observed at lysozyme and lysozyme-immobilized silica. The peak at 1530 cm^{-1}, corresponding to the amide II band [37], can also be clearly seen in lysozyme-immobilized silica. These spectral characteristics indicate that the secondary structure of the protein is maintained in the immobilized lysozyme

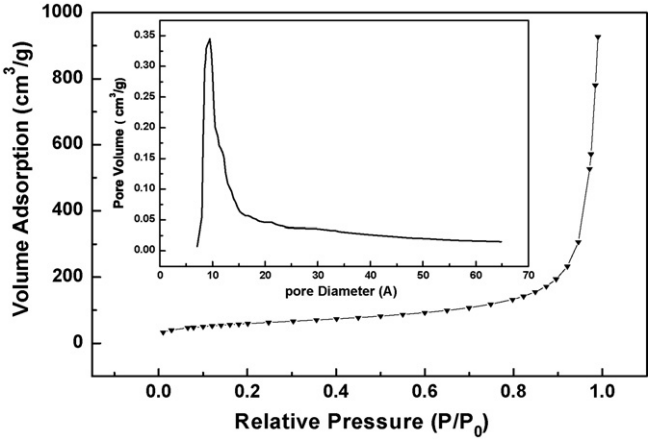

Fig. 3. N_2 adsorption isotherm for solid silica nanoparticles and the corresponding pore size distribution (inset).

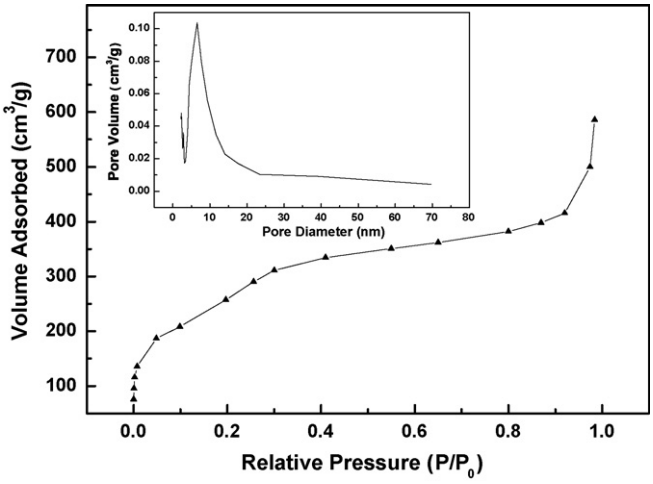

Fig. 4. N_2 adsorption isotherm for hollow silica nanotubes and the corresponding pore size distribution (inset).

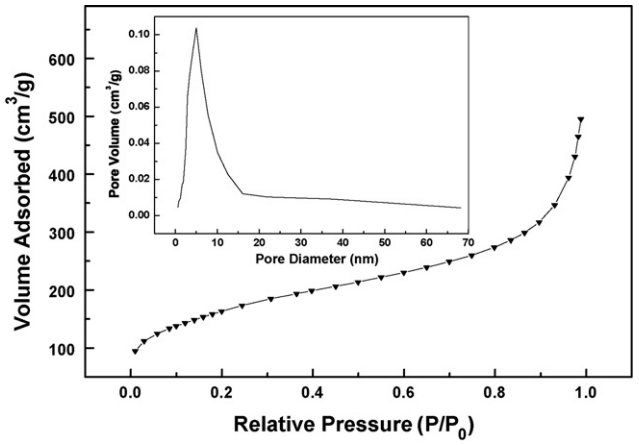

Fig. 5. N_2 adsorption isotherm for hollow silica nanospheres and the corresponding pore size distribution (inset).

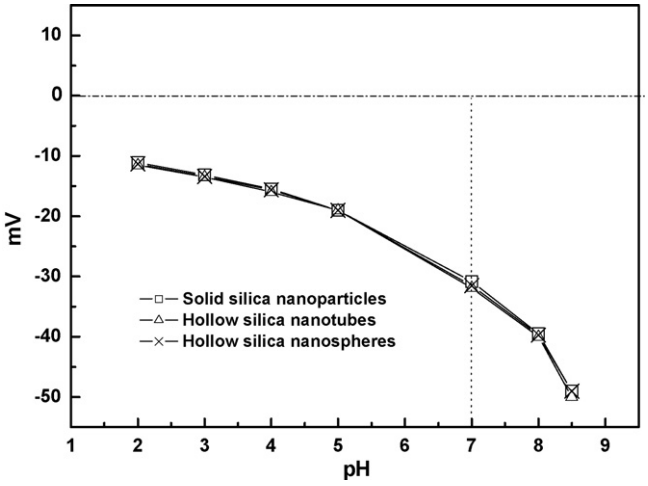

Fig. 6. The zeta potential curves of silica materials.

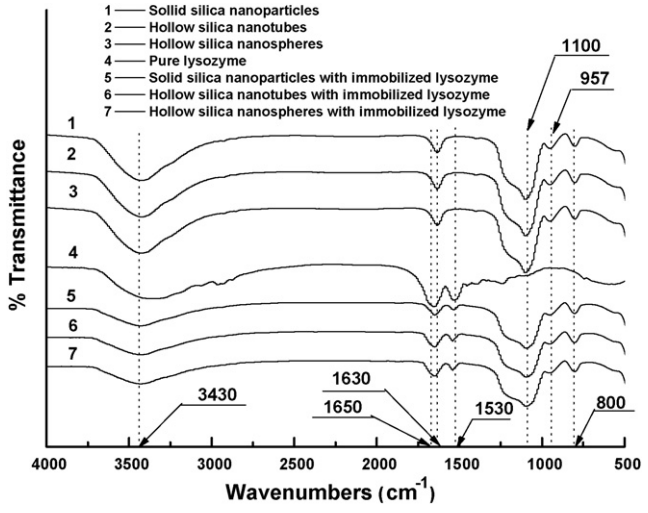

Fig. 7. FTIR spectra of silica materials, pure lysozyme and silica materials with immobilized lysozyme.

molecules and also indicate that as-prepared silica carriers are compatible with the physiological medium.

3.3. Immobilization of lysozyme on silica materials

Fig. 8 shows immobilization of lysozyme on silica nanoparticles at the same conditions. It can be seen that the amount of immobilized lysozyme within solid silica nanoparticles is 186 mg/g silica when lysozyme/silica ratio is 1:1, and while that of immobilized lysozyme within hollow silica nanotubes and hollow silica nanospheres could, respectively, reach up to 351 mg/g silica and 385 mg/g silica which is not only higher than the immobilization abilities of solid silica nanoparticles, but also higher than mesoporous silica (MPS) without designed structure and some surface-modified MPS [38]. From Fig. 8a, it can be seen that the adsorption of lysozyme onto solid silica nanoparticles involves only one stage and quickly reach to equilibrium. A possible reason is that the pore diameter (about 12.6 Å) of solid silica nanoparticles is too small and makes the molecules (about 3 nm) of lysozyme difficult to enter into the narrow channel of solid nanoparticles. From Fig. 8b and c, it was found that the adsorption process of lysozyme onto hollow silica materials could be divided into two stages. The first stage is mainly the adsorption of lysozyme onto the external surface of hollow silica materials, which occurs in a very short time of 60–80 min. The second stage is mainly comprised of both further adsorption of lysozyme inside the inner channel and encapsulation of lysozyme in the void space of hollow silica materials, which takes a much longer time to reach equilibrium.

So it can be concluded that good morphology and large pore size of silica materials would enhance the amount of immobilized lysozyme within silica materials. Furthermore, if the pore size of silica materials is smaller the molecular dimensions of enzymes, the bulky enzymes diffuse difficultly into the narrow channel of silica materials and the most of the surface areas of silica materials would not be utilized for enzymatic immobilization, which have been illuminated by the fact that the amount of immobilized lysozyme within solid silica nanoparticles is far

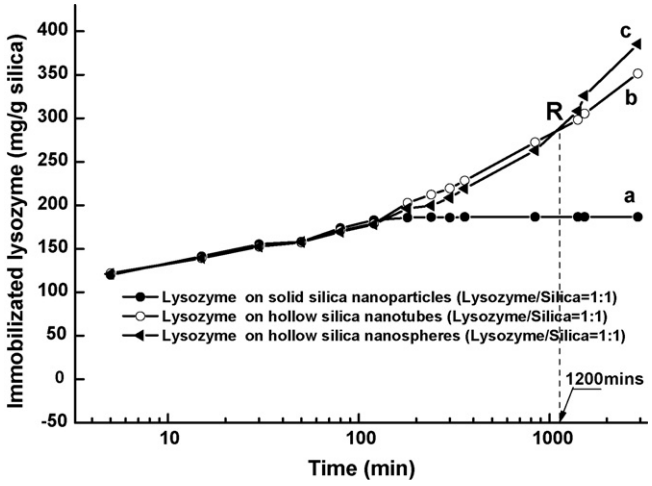

Fig. 8. Immobilization of lysozyme on silica materials.

lower than that of immobilized lysozyme within hollow silica nanoparticles.

3.4. Enzymatic catalysis

The enzymatic specific and relative activities are two of the most important parameters of the immobilized enzymes. The two parameters of lysozyme immobilized onto different silica materials were investigated and the results were presented in Fig. 9. Relative enzyme activity was determined as the specific activity ratio between immobilized and free enzyme. The enzymatic activity of the free lysozyme in solution is about 9600 unit/mg in the experiment. From Fig. 9, it can be seen that the specific activity of lysozyme immobilized onto solid silica nanoparticles is 1.08×10^6 unit/g, which is lower than those of lysozyme immobilized onto hollow silica nanotubes (1.46×10^6 unit/g) and onto hollow silica nanospheres (1.38×10^6 unit/g). The relative activity of lysozyme immobilized onto silica materials is 71.61% for solid silica, 58.70% for hollow silica nanotubes, and 51.64% for hollow silica nanospheres, respectively. The immobilized lysozyme molecules onto the three types of silica materials lose partly enzymatic activity due to adsorption on silica. Lysozyme immobilized onto solid silica nanoparticles possess the highest relative activity, which can be explained based on the fact that the lysozyme molecules were mainly adsorbed on the external surface of solid silica nanoparticles. While, therein, taking higher enzymatic specific activity into account, solid silica nanoparticles is not the most appropriate candidate for lysozyme immobilization. Although the amount of immobilized lysozyme on hollow silica nanotubes (351 mg/g silica) was lower than that of immobilized lysozyme on hollow silica nanospheres (385 mg/g silica) as mentioned above (see also Fig. 8), the relative activity of immobilized lysozyme exhibits an adverse trend, that is, the former (58.70%) is higher than that of immobilized lysozyme on the latter (51.64%). Possible reason for higher relative activity of immobilized lysozyme on hollow silica tubes is a relatively facile diffusion process of species across the shell walls due to their unique big entrances at the two ends (diameter of about 120–200 nm). But in a way the relatively airtight structure of hollow silica nanospheres would have an adverse effect on diffusion process.

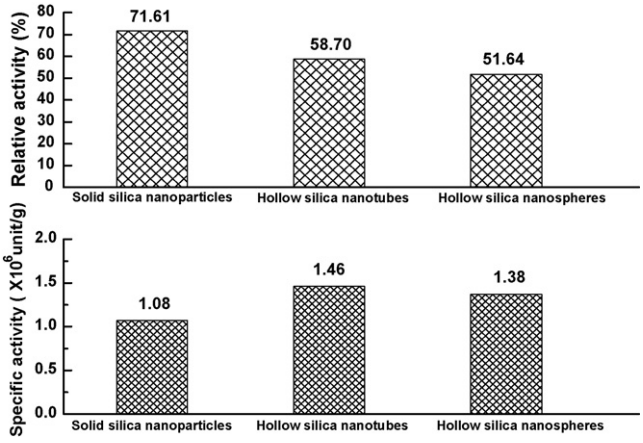

Fig. 9. Activity of immobilized lysozyme onto silica materials.

4. Conclusions

Solid silica nanoparticles, hollow silica nanotubes by using needle-like $CaCO_3$ templates, hollow silica nanospheres by using cuboidal $CaCO_3$ templates have been prepared successfully. The prepared silica materials were utilized for immobilization of lysozyme and are proved to be efficient for lysozyme immobilization in the adsorption experiment. Through the comparative study of immobilization of lysozyme onto the three different silica materials, we found that the adsorption process of lysozyme onto hollow silica materials could be divided into two stages. Good hollow structure and large pore size of silica materials would enhance the amount of immobilized large molecules, such as lysozyme, within silica materials. An interesting phenomenon is that the relatively airtight structure of hollow silica nanospheres has two contrasting effects on enzymatic immobilization. On one hand, the relatively airtight structure of hollow silica nanospheres is more useful for the molecules of lysozyme to be captured and restricted into the void space of silica nanospheres. Thus, this facilitates to enhance the amount of immobilized enzyme onto hollow silica nanospheres. But on the other hand, the relatively airtight structure might affect the diffusion/mass-transfer processes upon substrates entering in and products flowing out through the shell of hollow silica nanospheres, leading to the decrease of the immobilized lysozyme activity. The comparative study of immobilization of lysozyme onto the three different silica materials indicated clearly that hollow silica nanomaterials would be better potential candidates for enzyme immobilization than solid silica nanoparticles. We expect that hollow silica nanomaterials can be applicable as carriers for more versatile enzyme immobilization and macromolecule protection.

Acknowledgements

This work was supported by the National Natural Science Foundation of China (nos. 50642042, 20325621), the "973" program of China (no. 2003CB615807) and the Talent Training Program of the Beijing City (no. 9558103500).

References

[1] C.H. Jang, B.D. Stevens, P.R. Carlier, M.A. Calter, W.A. Ducker, Immobilized enzymes as catalytically-active tool for nanofabrication, J. Am. Chem. Soc. 124 (2002) 12114–12115.
[2] A.F. Abdel-Fattah, M.Y. Osman, M.A. Abdel-Naby, Production and immobilization of cellobiase from *Aspergillus niger* A20, Chem. Eng. J. 68 (1997) 189–196.
[3] C.M.F. Soares, M.H.A. Santana, G.M. Zanin, H.F. De Castro, Covalent coupling method for lipase immobilization on controlled pore silica in the presence of nonenzymatic proteins, Biotechnol. Prog. 19 (2003) 803–807.
[4] Y. Han, S.S. Lee, J.Y. Ying, Pressure-driven enzyme entrapment in siliceous mesocellular foam, Chem. Mater. 18 (2006) 643–649.
[5] A.S. Maria Chong, X.S. Zhao, Functionalized nanoporous silicas for the immobilization of penicillin acylase, Appl. Surf. Sci. 237 (2004) 398–404.

[6] P. Ye, Z.K. Xu, A.F. Che, J. Wu, P. Seta, Chitosan-tethered poly(acrylonitrile-*co*-maleic acid) hollow fiber membrane for lipase immobilization, Biomaterials 26 (2006) 6394–6403.
[7] C.H. Lei, Y.S. Shin, J. Liu, E.J. Ackerman, Entrapping enzyme in a functionalized nanoporous support, J. Am. Chem. Soc. 124 (2002) 11242–11243.
[8] R.B. Bhatia, C. Jeffrey Brinker, Aqueous sol–gel process for protein encapsulation, Chem. Mater. 12 (2000) 2434–2441.
[9] M. Miyazaki, J. Kaneno, R. Kohama, M. Uehara, K. Kanno, M. Fujii, H. Shimizu, H. Maeda, Preparation of functionalized nanostructures on microchannel surface and their use for enzyme microreactors, Chem. Eng. J. 101 (2004) 277–284.
[10] J. Fan, J. Lei, L.M. Wang, C.Z. Yu, B. Tu, D.Y. Zhao, Rapid and high-capacity immobilization of enzymes based on mesoporous silicas with controlled morphologies, Chem. Commun. 17 (2003) 2140–2141.
[11] L. Blasi, L. Longo, G. Vasapollo, R. Cingolani, R. Rinaldi, T. Rizzello, R. Acierno, M. Maffia, Characterization of glutamate dehydrogenase immobilization on silica surface by atomic force microscopy and kinetic analyses, Enzyme Microb. Technol. 36 (2005) 818–823.
[12] Y. Wei, J.G. Xu, Q.W. Feng, H. Dong, M. Lin, Encapsulation of enzymes in mesoporous host materials via the nonsurfactant-templated sol–gel process, Mater. Lett. 44 (2000) 6–11.
[13] A.S. Maria Chong, X.S. Zhao, Design of large-pore mesoporous materials for immobilization of penicillin G acylase biocatalyst, Catal. Today 93–95 (2004) 293–299.
[14] H. Takahashi, B. Li, T. Sasaki, C. Miyazaki, T. Kajino, Immobilized enzymes in ordered mesoporous silica materials and improvement of their stability and catalytic activity in an organic solvent, Micropor. Mesopor. Mater. 44/45 (2001) 755–762.
[15] H. Takahashi, B. Li, T. Sasaki, C. Miyazaki, T. Kajino, S. Inagaki, Catalytic activity in organic solvents and stability of immobilized enzymes depend on the pore size and surface characteristics of mesoporous silica, Chem. Mater. 12 (2000) 3301–3305.
[16] F. Miyaji, S.A. Davis, J.P.H. Charmant, S. Mann, Organic crystal templating of hollow silica fibers, Chem. Mater. 11 (1999) 3021–3024.
[17] A. Kowalski, M. Vogel, R.M. Blankenship, US Patent 4 427 836 (1984).
[18] M. Jafelicci Jr., M.R. Davolos, F.J. Santos, S.J. de Andrade, Hollow silica particles from microemulsion, J. Non-Cryst. Solids 247 (1999) 98–102.
[19] J. Hotz, W. Meier, Vesicle-templated polymer hollow spheres, Langmuir 14 (1998) 1031–1036.
[20] J.F. Chen, H.M. Ding, J.X. Wang, L. Shao, Preparation and characterization of porous hollow silica nanoparticles for drug delivery application, Biomaterials 25 (2004) 723–727.
[21] M. Hartmann, Ordered mesoporous materials for bioadsorption and biocatalysis, Chem. Mater. 17 (2005) 4577–4593.
[22] G.S. Zhu, S.L. Qiu, O. Terasaki, Y. Wei, Polystyrene bead-assisted self-assembly of microstructured silica hollow spheres in highly alkaline media, J. Am. Chem. Soc. 123 (2001) 7723–7724.
[23] P.M. Arnal, C. Weidenthaler, F. Schüth, Highly monodisperse zirconia-coated silica spheres and zirconia/silica hollow spheres with remarkable textural properties, Chem. Mater. 18 (2006) 2732–2739.
[24] J. Rubio Retama, B. Lopez-Ruiz, E. Lopez-Cabarcos, Microstructural modifications induced by the entrapped glucose in cross-linked polyacrylamide microgels used as glucose sensors, Biomaterials 24 (2003) 2965–2973.
[25] M.F. Gouzy, C. Sperling, T. Salchert, U. Streller, P. Uhlmann, C. Rauwolf, F. Simon, B. Voit, C. Werner, In vitro blood compatibility of polymeric biomaterials through covalent immobilization of an amidine derivative, Biomaterials 25 (2004) 3493–3501.
[26] Y.Q. Yeh, B.C. Chen, H.P. Lin, C.Y. Tang, Synthesis of hollow silica spheres with mesostructured shell using cationic-anionic-neutral block copolymer ternary surfactants, Langmuir 22 (2006) 6–9.
[27] A.D. Deng, M. Chen, S.X. Zhou, B. You, L.M. Wu, A novel method for the fabrication of monodisperse hollow silica spheres, Langmuir 22 (2006) 6403–6407.
[28] S.O. Obare, N.R. Jana, C.J. Murphy, Preparation of polystyrene- and silica-coated gold nanorods and their use as templates for the synthesis of hollow nanotubes, Nano Lett. 1 (2001) 601–603.
[29] D.T. Mitchell, S.B. Lee, L. Trofin, N.C. Li, T.K. Nevanen, H. Sderlund, C.R. Martin, Smart nanotubes for bioseparations and biocatalysis, J. Am. Chem. Soc. 124 (2002) 11864–11865.
[30] Q.G. Xiao, X. Tao, J.F. Chen, Silica nanotubes based on needle-like calcium carbonate: fabrication and immobilization for glucose oxidase, Ind. Eng. Chem. Res. 46 (2007) 459–463.
[31] L. Iucci, F. Patrignani, M. Vallicelli, E.G. Guerzoni, R. Lanciotti, Effects of high pressure homogenization on the activity of lysozyme and lactoferrin against listeria monocytogenes, Food Control 18 (2007) 558–565.
[32] J.F. Chen, J.X. Wang, R.J. Liu, L. Shao, L.X. Wen, Synthesis of porous silica structures with hollow interiors by templating nanosized calcium carbonate, Inorg. Chem. Commun. 7 (2004) 447–449.
[33] Q.G. Xiao, X. Tao, J.P. Zhang, J.F. Chen, Hollow silica nanotubes for immobilization of penicillin G acylase enzyme, J. Mol. Catal. B-Enzym. 42 (2006) 14–19.
[34] P. Xue, G.Z. Lu, Y.L. Guo, Y.S. Wang, Y. Guo, A novel support of MCM-48 molecular sieve for immobilization of penicillin G acylase, J. Mol. Catal. B-Enzym. 30 (2004) 75–81.
[35] A. Dong, P. Huang, Redox-dependent changes in beta-extended chain and turn structures of cytochrome c in water solution determined by second derivative amide I infrared spectra, Biochemistry 31 (1992) 182–189.
[36] J.F. Rabolt, F.C. Burns, N.E. Schlotter, J.D. Swalen, Anisotropic orientation in molecular monolayers by infrared spectroscopy, J. Chem. Phys. 78 (1983) 946–952.
[37] A. Gole, G. Thakar, M. Sastry, Protein diffusion into thermally evaporated lipid films: role of protein charge/mass ratio, Colloids Surf. B 28 (2003) 209–214.
[38] A. Katiyar, S. Yadav, P.G. Smirmiotis, N.G. Pinto, Synthesis and lysozyme adsorption of rod-like large-pore periodic mesoporous organosilica, Prog. Solid State Chem. 34 (2006) 13–20.